Title
INTERPRETATION OF KINETIC RATE DATA TAKEN IN A CHANNEL FLOW CELL

Authors
West, A.C
Newman, J.

Publication Date
1989

LBL-26621
Preprint

Lawrence Berkeley Laboratory
UNIVERSITY OF CALIFORNIA

Materials & Chemical Sciences Division

Submitted to Journal of the Electrochemical Society

Interpretation of Kinetic Rate Data Taken in a Channel Flow Cell

A.C. West and J. Newman

January 1989

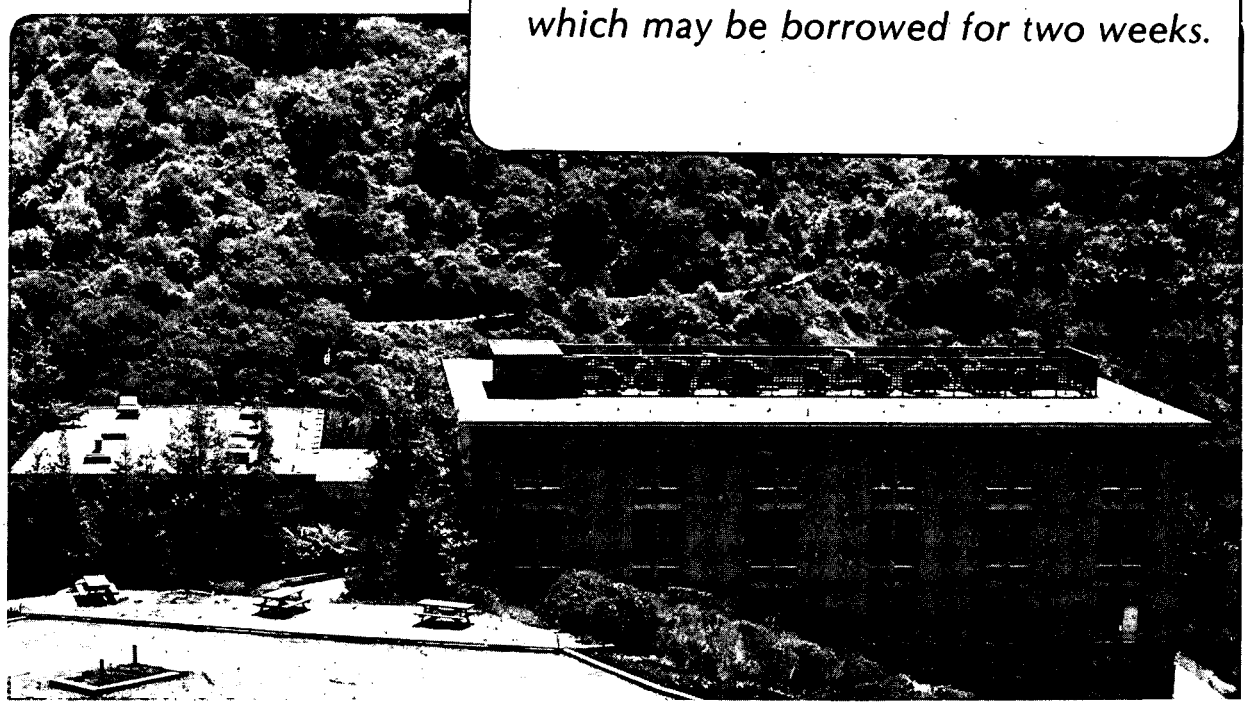

Prepared for the U.S. Department of Energy under Contract Number DE-AC03-76SF00098.

DISCLAIMER

LBL-26621

INTERPRETATION OF KINETIC RATE DATA TAKEN IN A CHANNEL FLOW CELL

Alan C. West and John Newman

Department of Chemical Engineering
University of California

and

Materials and Chemical Sciences Division
Lawrence Berkeley Laboratory
1 Cyclotron Road
Berkeley, CA 94720

LBL-26621

Interpretation of Kinetic Rate Data Taken in a Channel Flow Cell

Alan C. West and John Newman

Materials and Chemical Sciences Division, Lawrence Berkeley Laboratory,
and Department of Chemical Engineering, University of California,
Berkeley, California 94720

January 23, 1989

Abstract

Nonuniform current distributions can complicate the interpretation of kinetic rate measurements. This paper shows explicitly how nonuniformities affect measurements in the flow-channel cell. Results are given for linear and Tafel kinetics. In addition to the appropriate polarization parameter, the interpretation of data requires knowledge of the ratio of the two characteristic lengths and the placement of the reference electrode. The analysis assumes that the ohmic potential drop is subtracted from the measurements by the interruption of current and that concentration variations are negligible.

Key words: current distribution, linear kinetics, Tafel kinetics

Introduction

It has long been recognized that a nonuniform reaction distribution on an electrode can lead to difficulties in the interpretation of data [1]. Tiedemann *et al.* quantified this observation for the case of linear kinetic measurements on a disk electrode [2]. West and Newman [3] gave results for the more complicated case of Tafel kinetics on a disk electrode.

Measurements are also taken in the channel geometry. This geometry is useful because it has well-characterized (but nonuniform) mass-transfer rates. It may also be useful because of ease of construction.

The channel geometry has already been studied extensively; see especially, papers by Wagner [4] and by Parrish and Newman [5]. The key assumption of the analysis in this paper is that concentration variations can be neglected, which implies that $i_{avg} \ll \bar{i}_{lim}$, where $\bar{i}_{lim}$ is the average limiting current density. The validity of this assumption can be tested easily by calculating $\bar{i}_{lim}$ through knowledge of the transport properties and the flow conditions.

This geometry also approximates popular cell configurations used to study solid electrolytes. This analysis would be particularly applicable to these systems since, if the electrolyte contains only one charge carrier, concentration variations do not exist. It will also become evident that this analysis is especially relevant to solid electrolytes since their conductivities are often low (compared to aqueous solutions) and, hence, ohmic resistances are high.

The analysis of the channel geometry is more complicated than the analysis of the disk-electrode geometry because two characteristic lengths, shown in figure 1, are important. The ratios, h/L, of 1.0, 0.5, and 0.0 are investigated. Small values of h/L are chosen because small ratios tend to make current distributions more uniform and tend to reduce the ohmic drop of the cell.

It is assumed that the average surface overpotential is determined by the interruption of current. Additionally, the working electrode is assumed to be an anode, although the results can also be applied to the investigation of cathodic reactions. The counterelectrode is assumed to have the same kinetics as the working electrode, and the restrictiveness of this assumption is shown.

The emphasis of the results is on the placement of the reference electrode adjacent to the edge of the working electrode or *very far* from the electrode. To determine what can be considered *very far* from the working electrode, it is instructive to look at the primary potential distribution along the insulator, which is shown in figure 2. Within the resolution of the graph, the distribution for all three ratios of h/L is identical.

Analysis

The distribution of potential and current, in the absence of concentration variations, is governed by Laplace's equation and the appropriate boundary conditions. This analysis assumes that the working and counter electrodes are in the same reaction regime and have identical exchange current densities and transfer coefficients. Details of

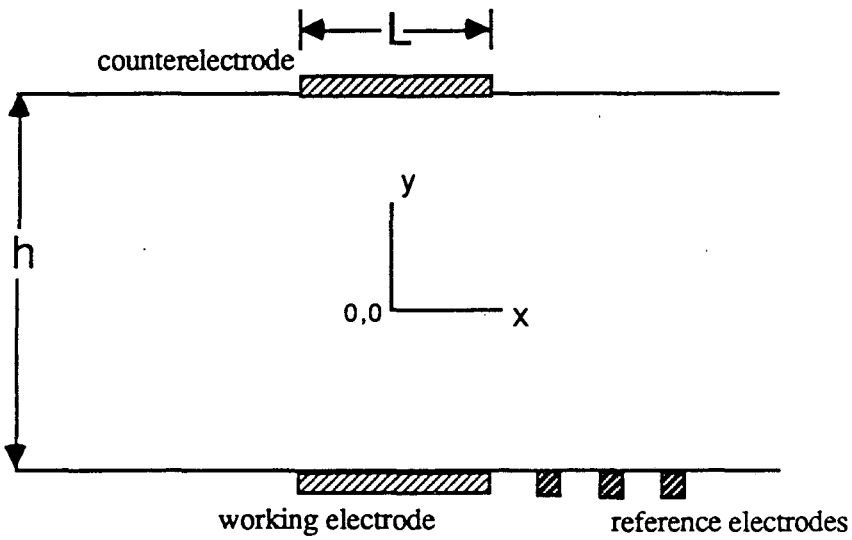

Figure 1. Cell geometry, showing the two characteristic lengths, the coordinate system, and possible reference electrode placements.

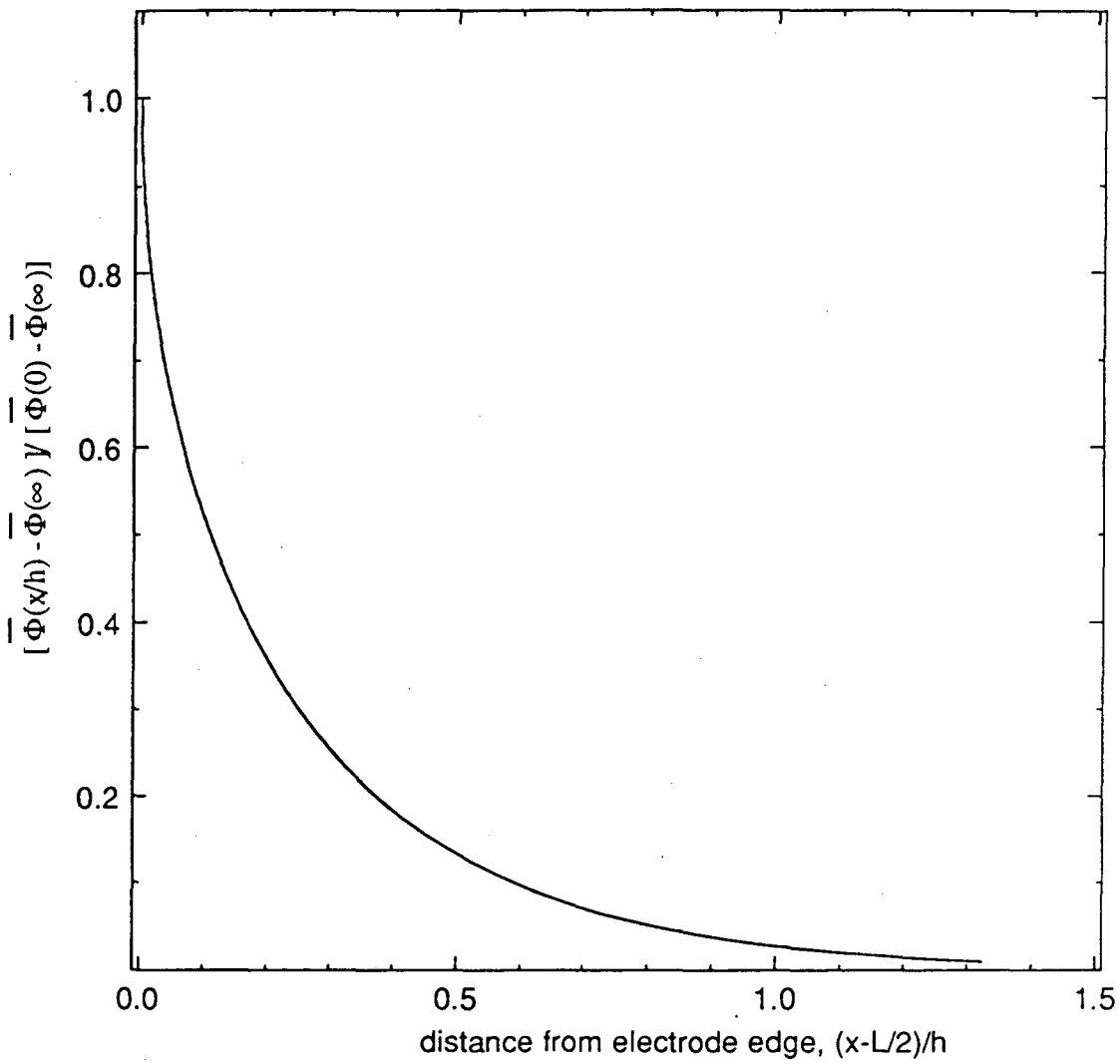

Figure 2. Primary potential distribution along the insulator, measured from the edge of the electrode, for h/L = 0, h/L = 0.5, and h/L = 1.0.

the solution procedure are given in the appendix.

In addition to the ratio of the characteristic lengths, it is necessary to specify the ratio of the ohmic to kinetic resistances to characterize completely how the data should be interpreted. Following Newman [6], the additional parameter for linear kinetics is

$$J = \frac{(\alpha_a+\alpha_c)Fhi_o}{RT\kappa} , \tag{1}$$

and for Tafel kinetics,

$$\delta = \frac{\alpha_a Fhi_{avg}}{RT\kappa} . \tag{2}$$

A nonuniform potential distribution on the electrode complicates the interpretation of data taken with the aid of a current interrupter method. An apparent surface overpotential determined by this method is given by [7]

$$\eta_{s,app} = V - \Phi(x,y) - \bar{\Phi}(0,h/2) + \bar{\Phi}(x,y), \tag{3}$$

where $\Phi(x,y)$ is the potential of the reference electrode,[†] and $\bar{\Phi}(0,h/2) - \bar{\Phi}(x,y)$ is the change in potential after the interruption of current and corresponds to the potential drop for a primary distribution with the same average current density.

Linear Kinetics Results

The rate of a reaction occurring in the linear kinetics regime is given by

---

[†]The reference electrode is assumed to be the same kind as the working electrode, but passes no current, and is in equilibrium with the solution.

$$i = \frac{i_o(\alpha_a+\alpha_c)F\eta_s}{RT} , \tag{4}$$

where $\eta_s = V - \Phi(x,h/2)$. Assuming that $\alpha_a+\alpha_c$ is known, one can determine an apparent exchange current density by specifying that

$$i_{avg} = \frac{i_{o,app}(\alpha_a+\alpha_c)F\eta_{s,app}}{RT} . \tag{5}$$

Combining equations (4) and (5) gives

$$\frac{i_o}{i_{o,app}} = \frac{i_o\eta_{s,app}}{i_{avg}} . \tag{6}$$

For a reference electrode adjacent to the edge of the electrode, equation (6) reduces to

$$\frac{i_o}{i_{o,app}} = \frac{i_{edge}}{i_{avg}} . \tag{7}$$

Results obtained from equation (6) and the numerical procedure described in the appendix are shown in figures 3 and 4 for various reference electrode placements. J_{app} is introduced to facilitate the use of these figures and is defined by

$$J_{app} = \frac{(\alpha_a+\alpha_c)Fhi_{o,app}}{RT\kappa} . \tag{8}$$

Tafel Kinetics Results

The important parameter for the characterization of Tafel kinetics is a dimensionless average current density. Since the proper interpretation of the data changes with the polarization parameter, a Tafel plot of data should not be expected to fall on a straight line, even if the Tafel equation exactly describes the kinetics of the reaction. This complicates the analysis for Tafel kinetics.

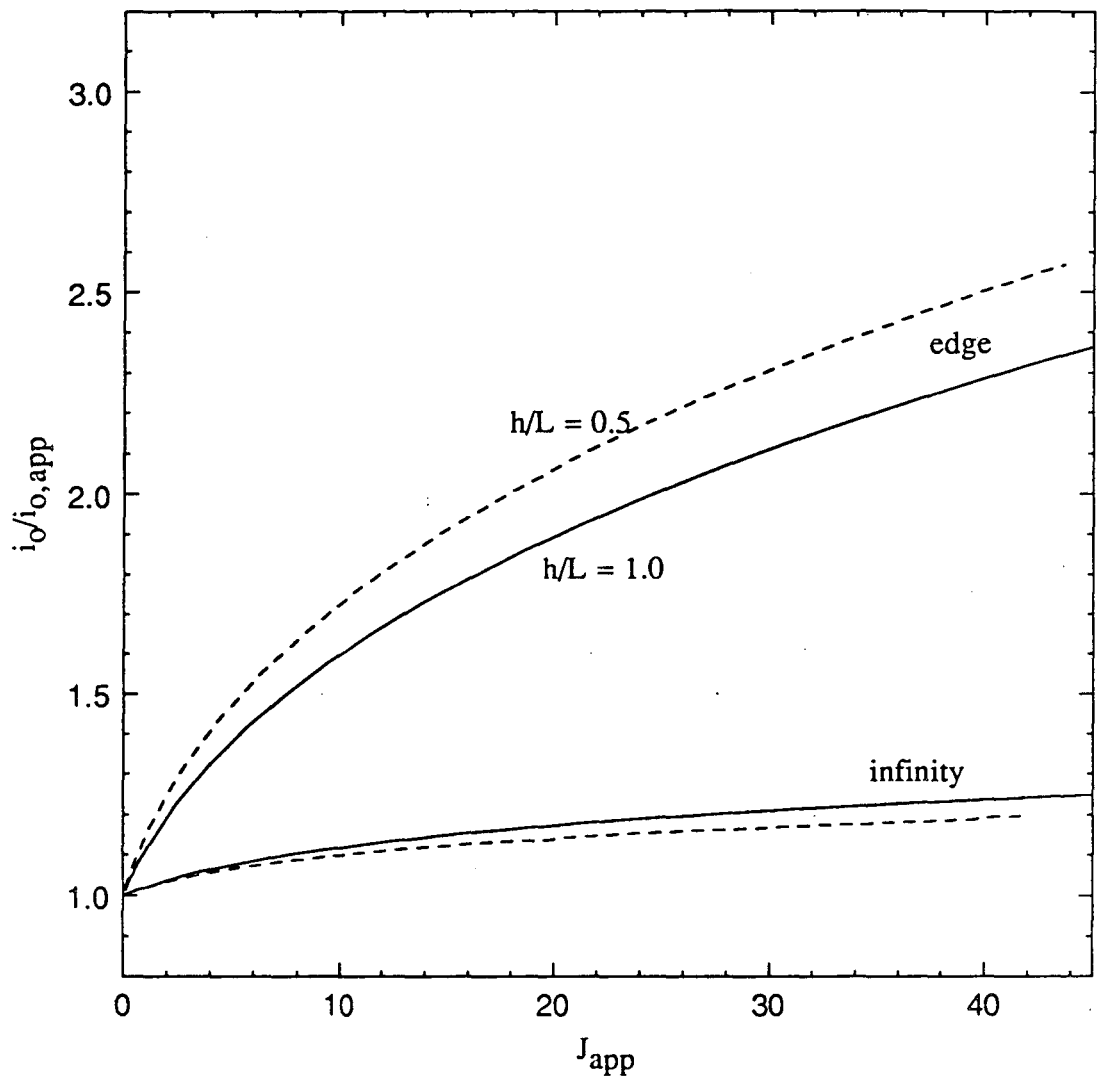

Figure 3. Correction factor for the exchange current density for linear kinetics for a reference electrode placed adjacent to the working electrode and for one placed very far from the working electrode.

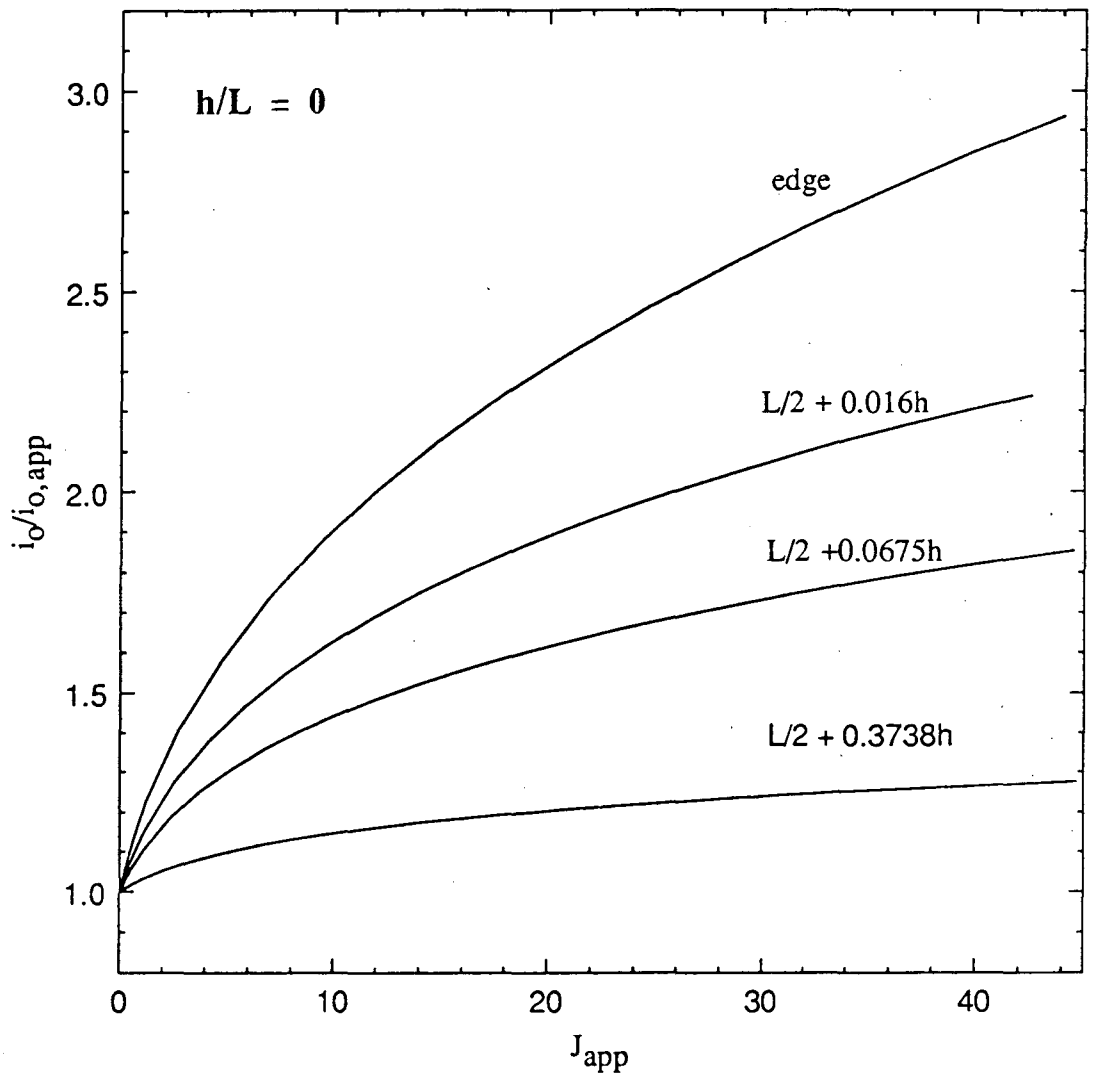

Figure 4. Correction factor for the exchange current density for linear kinetics, h/L = 0, and four reference electrode placements.

Reaction rates described by Tafel kinetics are given by

$$i = i_o \exp\left(\frac{\alpha_a F \eta_s}{RT}\right) . \tag{9}$$

Since local current densities and local surface overpotentials are not measurable, apparent kinetic parameters must be defined and should be related to measured quantities:

$$i_{avg} = i_{o,app} \exp\left(\frac{\alpha_{a,app} F \eta_{s,app}}{RT}\right) . \tag{10}$$

As West and Newman [3] discuss, a desired procedure for analyzing data is to define more precisely $i_{o,app}$ as the apparent exchange current density obtained when a line of slope $RT/\alpha_a F$ is fitted through the experimental data. It is, therefore, most interesting to report values of $i_o/i_{o,app}$ for the case of $\alpha_a = \alpha_{a,app}$. With this assumption, equations (9) and (10) give

$$\frac{i_o}{i_{o,app}} = \frac{i_o}{i_{avg}} \exp\left(\frac{\alpha_a F \eta_{s,app}}{RT}\right) . \tag{11}$$

For the case of a reference electrode adjacent to the edge of the working electrode, equation (11) reduces to equation (7). Results for various reference electrode placements are shown in figures 5 and 6.

Before i_o can be obtained from $i_{o,app}$, it is necessary to know α_a, which can be determined from $\alpha_{a,app}$:

$$\alpha_{a,app} = \frac{RT}{F} \frac{d\ln i_{avg}}{d\eta_{s,app}} . \tag{12}$$

Combining equations (11) and (12) gives

$$\frac{\alpha_a}{\alpha_{a,app}} = 1 + \left[\frac{d\ln(i_o/i_{o,app})}{d\ln\delta}\right]_{\alpha_a=\alpha_{a,app}} , \tag{13}$$

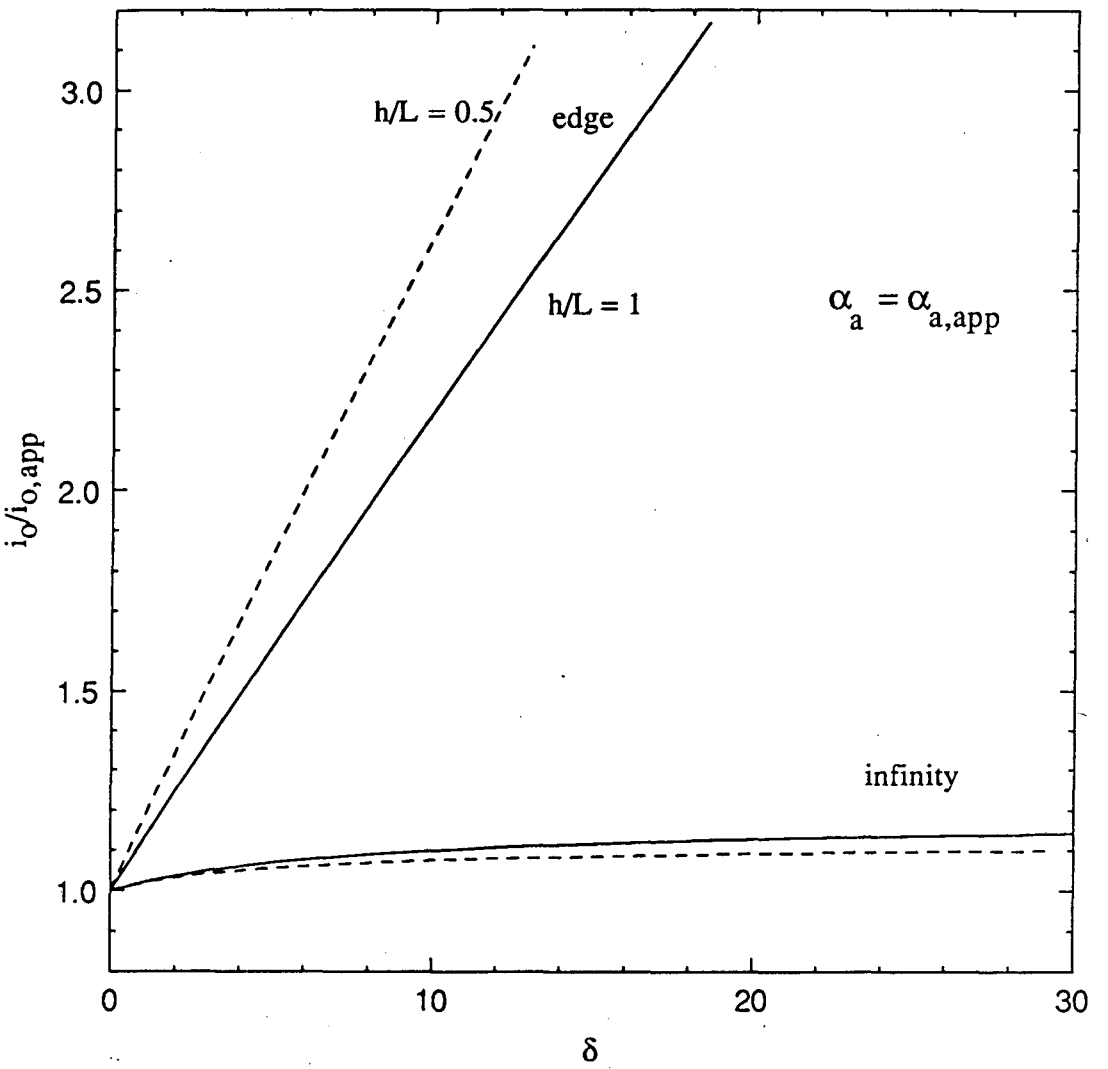

Figure 5. Correction factor for the exchange current density for Tafel kinetics, two reference electrode placements, and two ratios of h/L.

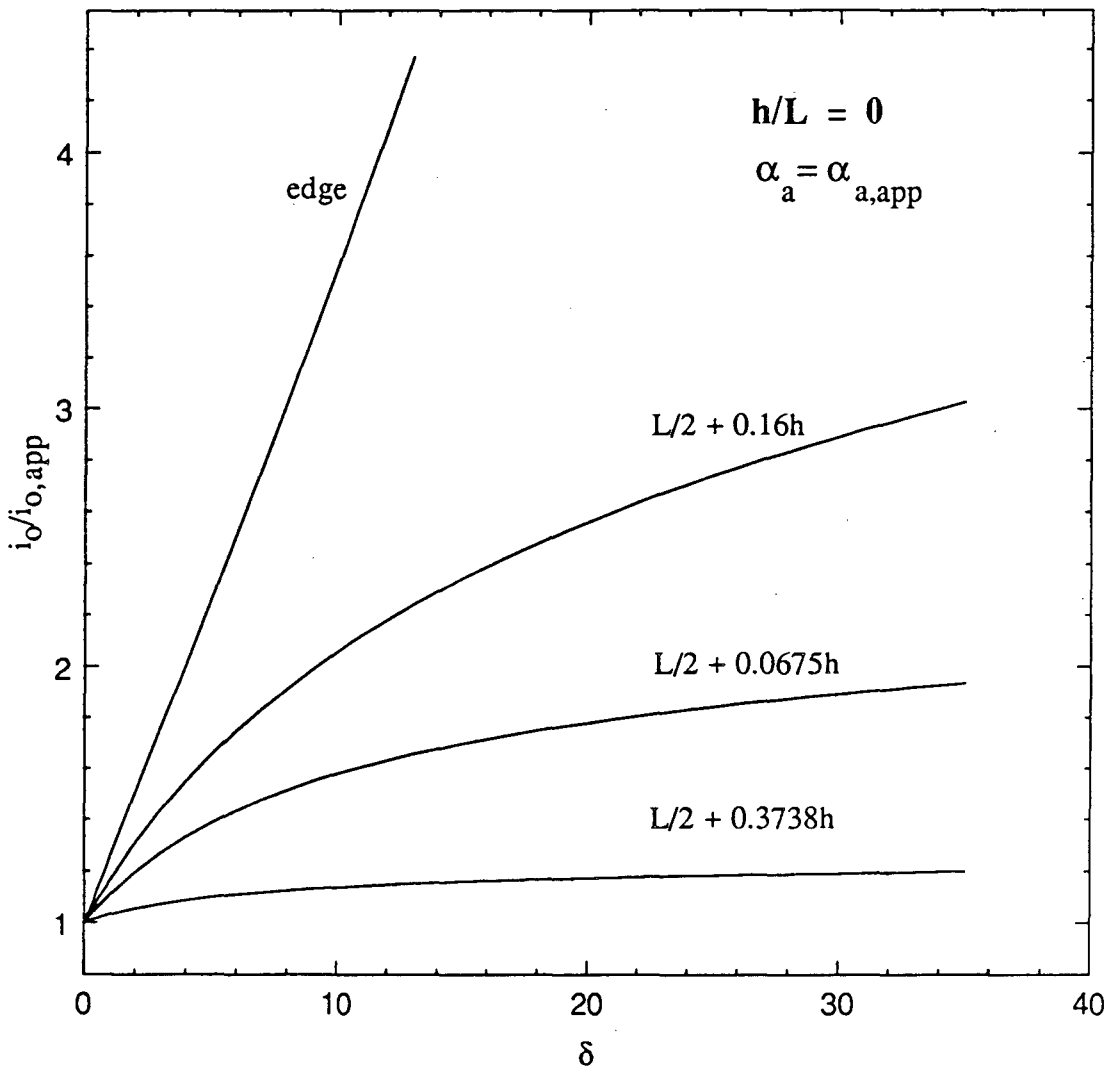

Figure 6. Correction factor for the exchange current density for Tafel kinetics, h/L = 0, and four reference electrode placements.

where the right side of equation (13) is to be evaluated assuming that $\alpha_a = \alpha_{a,app}$. Equation (13) was evaluated by differentiating fourth-degree polynomials which were fitted to logarithmic plots of the results displayed in figures 5 and 6. Results are shown in figures 7 and 8, where δ_{app} is given by

$$\delta_{app} = \frac{\alpha_{a,app} Fhi_{avg}}{RT\kappa} , \tag{14}$$

and is introduced to make easier the determination of α_a from these figures.

Precisely determining i_o and α_a from Tafel data can be difficult. The procedure that one might take is outlined as follows:

1. Determine $\alpha_{a,app}$ from the slope of the data ($\ln i_{avg}$ *vs.* $\eta_{s,app}$).
2. Calculate δ_{app} from the value of i_{avg} at which the "apparent" Tafel slope was determined.
3. Obtain α_a from figure 7 or 8.
4. Determine $i_{o,app}$ from a line with the correct Tafel slope drawn through the value of i_{avg} used to calculate δ_{app}..
5. Use figure 5 or 6 to calculate i_o.

Discussion

Figure 3 shows $i_o/i_{o,app}$ for linear kinetics. As can be expected [2], the correction to $i_{o,app}$ can be much lower for a reference electrode placed at infinity. Unfortunately, it is not always possible to place the reference electrode far from the working electrode because the ohmic potential may dominate the measurements.

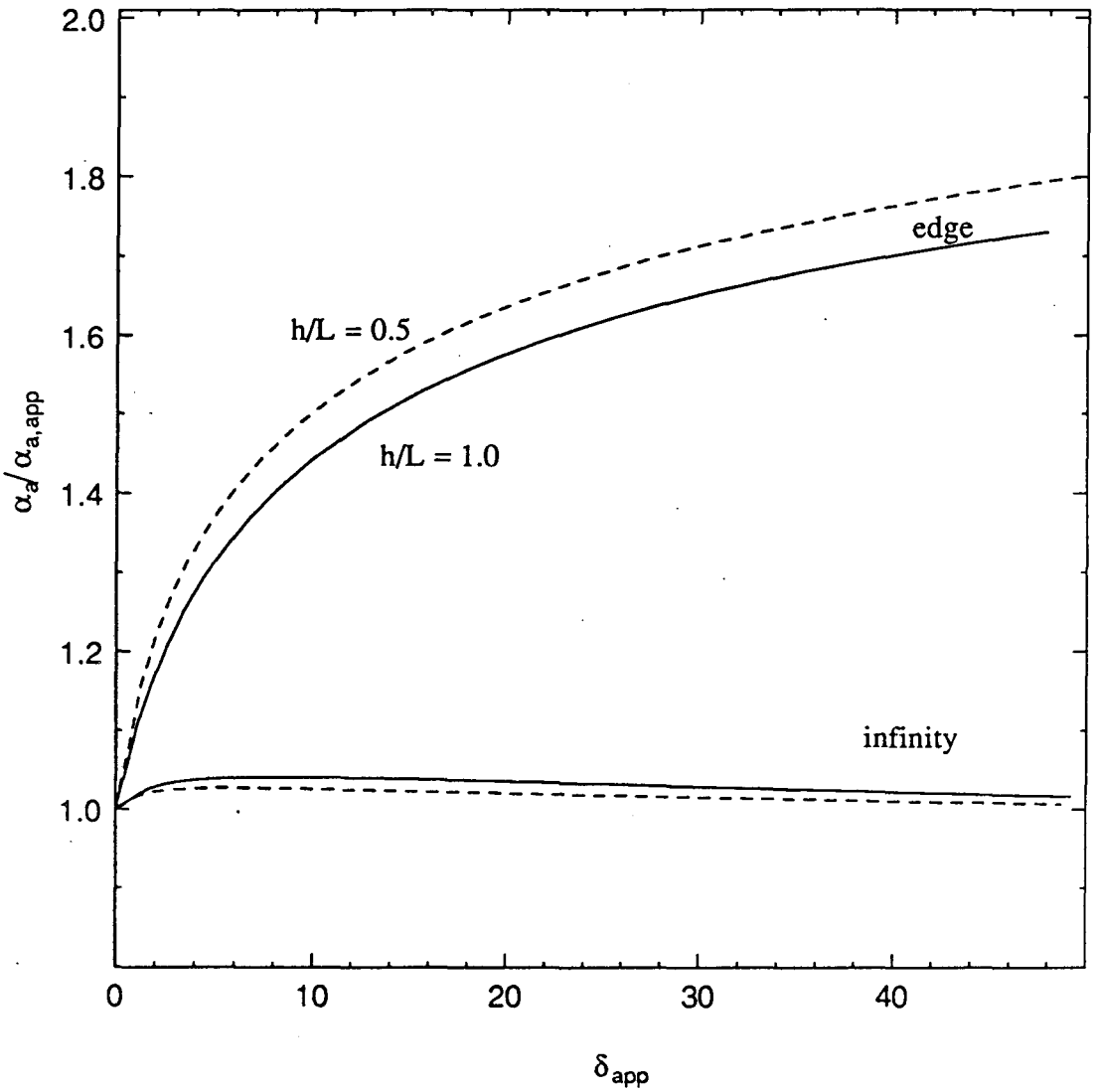

Figure 7. Correction factor for the transfer coefficient as a function of the apparent dimensionless average current density for two reference electrode placements and two ratios of h/L.

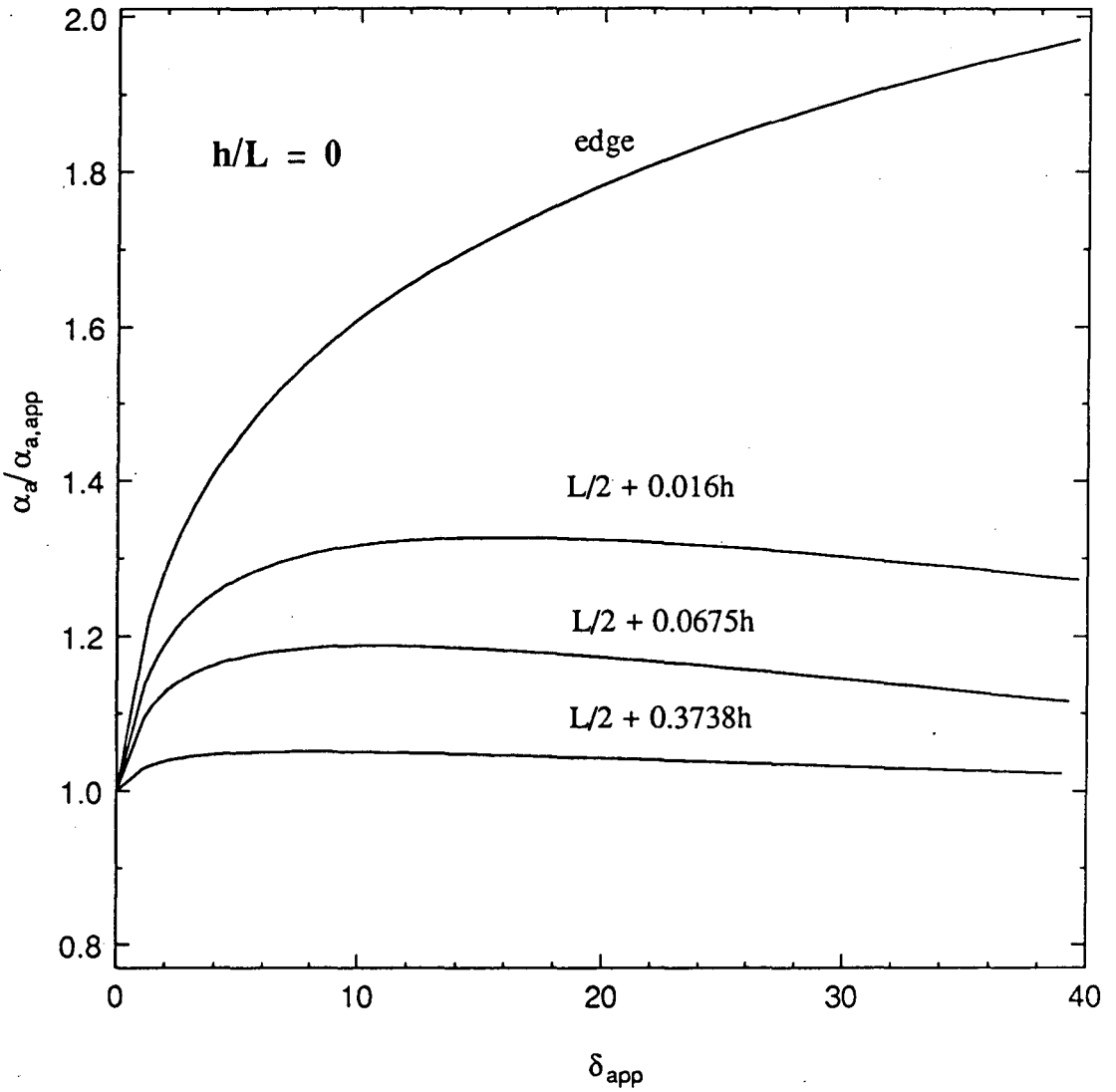

Figure 8. Correction factor for the transfer coefficient as a function of the apparent dimensionless average current density for h/L = 0 and for various positions of the reference electrode.

For a reference electrode placed adjacent to the working electrode, the errors are greater (for a given J) for the smaller ratio, h/L. This result is surprising because a smaller ratio should decrease the necessary correction. This apparent inconsistency is explained by realizing that the choice of h in the definition of J is arbitrary, and perhaps L would be a more physically significant length in describing the ratio of the ohmic to kinetic resistances. This is indeed true as $h/L \longrightarrow \infty$. ($h$ was used in the definition of J because it is the important length in the limit as $h/L \longrightarrow 0$.)

Figure 4 shows $i_o/i_{o,app}$ for linear kinetics and $h/L = 0$. For this ratio, errors are always zero for a reference electrode placed at infinity. Three intermediate reference electrode placements are also given. These particular positions were chosen because they correspond to the positions along the insulator where the primary potential difference, $\bar{\Phi}(0,h/2) - \bar{\Phi}(x,h/2)$, is twenty, forty, and eighty percent of $\bar{\Phi}(0,h/2) - \bar{\Phi}(\infty,h/2)$.

Figures 5 and 6 show $i_o/i_{o,app}$ for Tafel kinetics. As West and Newman discuss [3], a Tafel plot of data can not be extended through $\delta = 0$ because the cathodic term of the Butler-Volmer equation becomes important. $i_{o,app}$, then, is determined by extrapolating a line of slope $RT/\alpha_a F$ through the Tafel portion of the data. A point near which the data deviate from this Tafel slope determines the value of δ which is used to obtain the appropriate correction factor to $i_{o,app}$.

Figures 7 and 8 show $\alpha_a/\alpha_{a,app}$. As $\delta \longrightarrow 0$, $\alpha_a = \alpha_{a,app}$ for any reference electrode placement. For a reference electrode placed adjacent to the edge of the working electrode, $\alpha_a = 2\alpha_{a,app}$ as $\delta \longrightarrow \infty$. This

is the same as the result obtained for the rotating disk electrode. Smyrl and Newman [8] show that this result holds for any reference electrode placed at the edge of a *coplanar* electrode and insulator. For any other reference electrode placement, $\alpha_a = \alpha_{a,app}$ as $\delta \longrightarrow \infty$.

Results from West and Newman [9] can be used to show that, for a reference electrode placed next to an electrode/insulator edge, $\alpha_a/\alpha_{a,app} = 2\beta/\pi$ as $\delta \longrightarrow \infty$, where β is the interior angle between the electrode and insulator. Their results can also be used to show that, for linear kinetics, $i_o \propto i_{o,app}^{2\beta/\pi}$ as $J \longrightarrow \infty$, for a reference electrode placed adjacent to the edge. For Tafel kinetics, $i_o \propto i_{o,app} \cdot i_{avg}^{2\beta/\pi-1}$ as $\delta \longrightarrow \infty$.

For all of the results in this analysis, it is assumed that both the counter and working electrodes are in the same reaction regime and have identical values for the kinetic parameters. Figure 9 is meant to indicate how restrictive this assumption is. It shows $i_o/i_{o,app}$ for a reference electrode placed adjacent to the working electrode for Tafel kinetics and for a counterelectrode with very fast kinetics, very slow kinetics, and with identical kinetics to the working electrode. For other reference electrode placements, the differences should be smaller.

Conclusions

Results are given for the interpretation of kinetic rate measurements taken in the linear and Tafel kinetics regimes. They indicate that reference electrodes should be placed far from the electrode. Because the ohmic overpotential can dominate the potential measurements, it is sometimes necessary to place the reference electrode near the

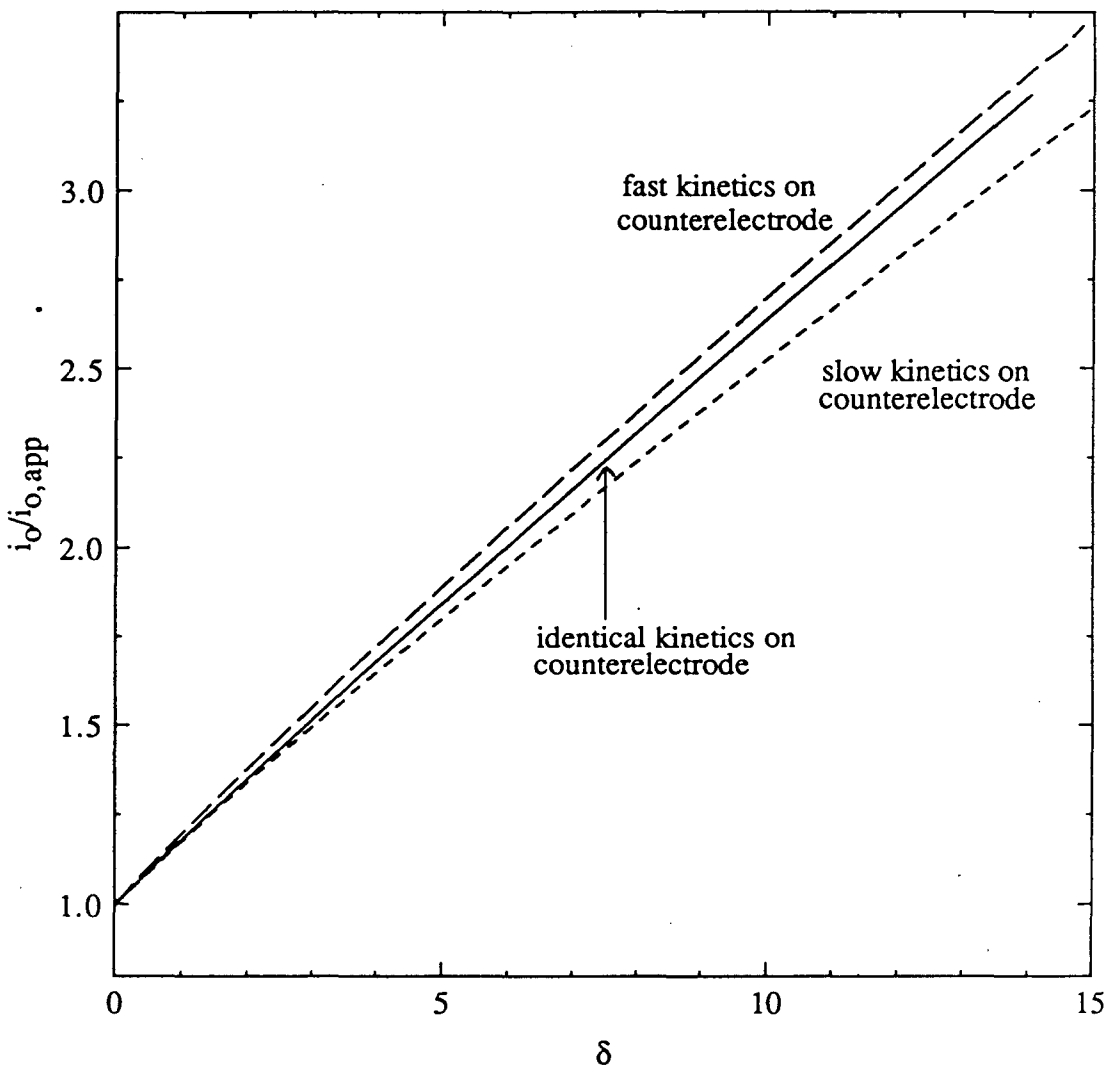

Figure 9. Correction factor to the exchange current density for a reference electrode placed adjacent to the working electrode for h/L = 0.5 and slow kinetics, identical kinetics, and fast kinetics on the counterelectrode.

working electrode.

A final observation worth noting is that uncertainty in the exact placement of the reference electrode will cause greater uncertainties in the interpretation of data for reference electrode placements closer to the working electrode. This is most obviously seen in figure 8 and can be explained completely by figure 2, which shows that the largest changes in potential occur near the working electrode.

Appendix

Boundary integral methods are useful for solving Laplace's equation [4], [10]. These techniques are discussed elsewhere [10], [11] and will not be elaborated on. To facilitate the use of the numerical procedure, the channel geometry was mapped conformally into the geometries shown in figure 10. Newman [12], [13] followed a similar procedure, except that he mapped the two electrodes so that they were coplanar (which is an intermediate Schwarz-Christoffel transformation used in the conformal mapping given here).

To solve for the current and potential distributions in the transformed geometry, the boundary conditions along the electrodes are (for finite h/L)

$$\frac{d\Phi}{dv_r} = f(\Phi_o)\, g_v(v_i), \tag{15}$$

where $f(\Phi_o)$ is given by the right side of equation (4) or (9), and

$$g_v(v_i) = -\frac{h}{\pi}\left[\cosh^2\epsilon_i - w^2\right]^{\frac{1}{2}}, \tag{16}$$

where

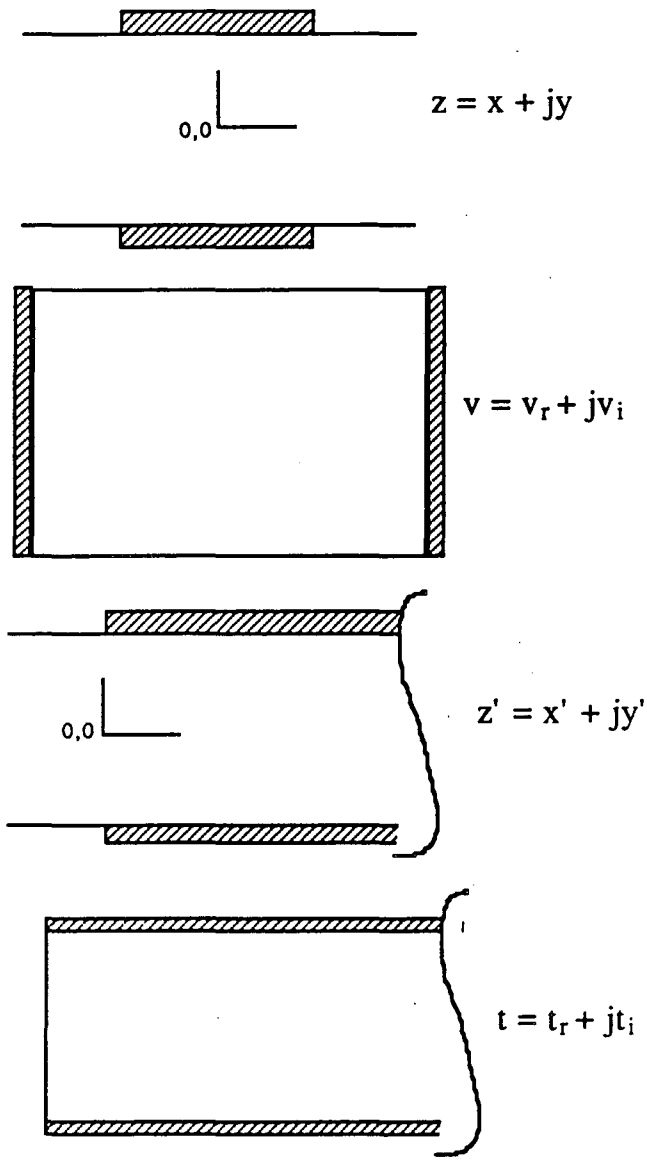

Figure 10. Original and transformed geometries, showing the working and counter-electrodes.

$$w = -j \sinh\left(\frac{\pi z}{h}\right) \tag{17}$$

and

$$\epsilon = \frac{\pi L}{2h} . \tag{18}$$

v is related to w through

$$v = -\int_0^w \frac{dw}{(w^2-1)^{1/2}\,(w^2-\cosh^2\epsilon)^{1/2}} . \tag{19}$$

For $h/L = 0$, the boundary condition along the electrode is given by

$$\frac{d\Phi}{dt_i} = f(\Phi_o)\, g_t(t_r) , \tag{20}$$

and $g_t(t_r)$ is given by

$$g_t(t_r) = -\frac{h}{\pi}\left(1 - e^{-2\pi x'}\right)^{1/2} . \tag{21}$$

t is related to z' through

$$t = \sin^{-1}\exp\left(\frac{\pi z'}{h}\right) . \tag{22}$$

z' is related to the original coordinate system by a shift in the origin.

The advantage of using conformal mapping prior to the boundary integral technique is that the mapping tends to provide automatically a mesh spacing appropriate for a given geometry. It can also reduce the time necessary for programming a new problem because many geometries can be mapped into one.

Acknowledgements

This work was supported by the Assistant Secretary for Conservation and Renewable Energy, Office of Energy Storage and Distribution, Energy Storage Division, U. S. Department of Energy under Contract No. DE-

AC03-76SF00098.

List of Symbols

F	Faraday's constant, 96487 C/equiv
g_t, g_v	functions relating derivatives in the transformed and original coordinate systems
h	interelectrode distance, cm
i	current density, A/cm^2
i_o	exchange current density, A/cm^2
$\bar{i}_{lim}$	average limiting current density, A/cm^2
j	$\sqrt{-1}$
J	dimensionless exchange current density
L	electrode length, cm
R	universal gas constant, 8.3143 J/mol-K
T	absolute temperature, K
t, v, w, z, z'	complex coordinates
V	electrode potential, V
x,y	cartesian coordinates, cm
x', y'	modified coordinate system for h/L = 0, cm
α_a, α_c	transfer coefficients
β	interior angle between insulator and electrode, radians
δ	dimensionless average current density
ϵ	ratio defined by equation (18)
η_s	surface overpotential, V
κ	specific conductivity, $\Omega^{-1}cm^{-1}$

π	3.141592654
Φ	solution potential, V
$\bar{\Phi}$	primary solution potential, V

Subscripts

app	apparent
avg	average
edge	electrode/insulator interface

References

[1] John Newman, "Current Distribution on a Rotating Disk below the Limiting Current," *J. Electrochem. Soc.*, **113**, 1235 (1966).

[2] W. H. Tiedemann, J. Newman, and D. N. Bennion, "The Error in Measurements of Electrode Kinetics Caused by Nonuniform Ohmic-Potential Drop to a Disk Electrode," *J. Electrochem. Soc.*, **120**, 256 (1973).

[3] Alan C. West and John Newman, "Corrections to Kinetic Measurements Taken on a Disk Electrode," *J. Electrochem. Soc.*, **136**, 139 (1989).

[4] Carl Wagner, "Theoretical Analysis of the Current Density Distribution in Electrolytic Cells," *J. Electrochem. Soc.*, **98**, 116 (1951).

[5] W. R. Parrish and John Newman, "Current Distributions on Plane, Parallel Electrodes in Channel Flow," *J. Electrochem. Soc.*, **117**, 43 (1970).

[6] John S. Newman, *Electrochemical Systems*, Prentice-Hall, Englewood Cliffs, N. J. (1973).

[7] John Newman, "Ohmic Potential Measured by Interrupter Techniques," *J. Electrochem. Soc.*, **117**, 507 (1970).

[8] William H. Smyrl and John Newman, "Current Distribution at Electrode Edges at High Current Densities," *J. Electrochem. Soc.*, **136**, 132 (1989).

[9] Alan C. West and John Newman, "Current Distribution Near an Electrode Edge as a Primary Distribution is Approached," *J. Electrochem. Soc.*, in press.

[10] C. A. Brebbia, *The Boundary Element Method for Engineers*, John Wiley and Sons, New York (1978).

[11] P. K. Banerjee and R. Butterfield, *Boundary Element Methods for Engineering Science*, McGraw-Hill, Inc., New York (1981).

[12] John Newman, "Engineering Design of Electrochemical Systems," *Ind. Eng. Chem.*, **60**, no. 4, 12 (1968).

[13] John Newman, "The Fundamental Principles of Current Distribution and Mass Transport in Electrochemical Systems," in *Electroanalytical Chemistry*, A. J. Bard, Editor, pp. 187-351, Marcel-Dekker, Inc., New York (1973).

LAWRENCE BERKELEY LABORATORY
TECHNICAL INFORMATION DEPARTMENT
UNIVERSITY OF CALIFORNIA
BERKELEY, CALIFORNIA 94720